J. Quant. Spectrosc. Radiat. Transfer, Vol. 19, pp. 51–62. Pergamon Press 1978. Printed in Great Britain

FAR-INFRARED ABSORPTION IN H_2 AND H_2–HE MIXTURES†

GEORGE BIRNBAUM‡
Science Center, Rockwell International, Thousand Oaks, CA 91360, U.S.A.

and

Institute for Materials Research, National Bureau of Standards, Washington, DC 20234, U.S.A.

(*Received* 5 *April* 1977)

Abstract—Collision-induced absorption in the translation-rotation band of H_2 and H_2–He mixtures has been measured from 20 to 900 cm^{-1} at 77.4, 195 and 292 K. To establish the accuracy of the results, various sources of error are investigated. The zeroth and first spectral moments are evaluated from experiment and theory for H_2 at the various temperatures. To obtain theoretical moments consistent with the experimental values, the quantum pair-distribution function must be used. The major portion of the experimental moments can be accounted for by quadrupole-induced dipoles in H_2 pairs. The remaining portion is attributable to an anisotropic overlap interaction, although its magnitude depends on the value of the molecular parameters required to calculate the quadrupole contribution.

1. INTRODUCTION

THE PRINCIPAL constituent of the atmosphere of the outer planets is molecular hydrogen, with helium presumed to be present in roughly comparable amounts.[1] The thermal emission from these atmospheres, with temperatures roughly from 80 to 160 K, is primarily in the far-i.r. region. Consequently, the dominant source of thermal opacity arises from rotational transitions at roughly 370 and 600 cm^{-1} and translational transitions extending from 0 to 500 cm^{-1} and higher due to transient dipoles induced in H_2–H_2 and H_2–He collisions.[2] The analysis of this thermal emission can yield significant information regarding the composition and temperature of planetary atmospheres provided the spectral intensity and band shape have been established from laboratory measurements. Although the absorption coefficient of gaseous equilibrium hydrogen (eH_2) has been measured at 85 K and normal H_2 (nH_2)§ at 195 K from 300 to 1400 cm^{-1},[3–5] no data are available on eH_2–He mixtures in this temperature and frequency range. Moreover, no data have been obtained in the translational part of the spectrum below 300 cm^{-1} in eH_2 and eH_2–He.

It is the purpose of this investigation to determine accurately the absorption coefficient of eH_2 and eH_2–He in the range 20–900 cm^{-1} at 77, 195 and 292 K.[2a] Although some data are available above 300 cm^{-1} it was worthwhile repeating these measurements because of discrepancies in previous results. For this reason, because of a number of unusual features in the experiment, and the importance of the results for the study of planetary atmospheres and molecular interactions, we present a full account of the measurements and the sources of error. The zeroth and first experimental spectral moments of H_2 are evaluated at the various temperatures and compared with the theoretical moments. These are calculated on the basis of quadrupole-induced dipoles in molecular pairs. To obtain reasonable agreement with the experimental values, the quantum pair distribution function must be used. These results are used to evaluate the anisotropic overlap contribution to the induced dipole in H_2 pairs.

2. EXPERIMENTAL ARRANGEMENT‖

(a) *Monochromator*

Spectra were obtained with a grating spectrometer[6] whose previous range 10–600 cm^{-1} was extended to higher frequencies by using a grating blazed in first order at 750 cm^{-1} with 384

†This work was supported, in part, by the Jet Propulsion Laboratory Contract Nos. 953284 and 953906, and NASA contract No. NAS5-20820.

‡Presently at the National Bureau of Standards, Washington, D. C. The measurements reported here were performed at Science Center, Rockwell International.

§Normal H_2, which is practically obtained in equilibrium at room temperature, is composed of 1/4 para-hydrogen and 3/4 ortho-hydrogen.

‖Certain commercial apparatus are identified to specify adequately the experimental procedure. In no case does such identification constitute a recommendation or endorsement by the National Bureau of Standards or Rockwell International.

lines/cm (PTR Optics). To remove radiation at frequencies corresponding to higher grating orders, an OCLI low-pass filter No. L-13510-9 was used from 450 to 700 cm^{-1} and No. L-07540-9 from 700 to 900 cm^{-1}. These filters, combined with a low-pass filter located in front of the bolometer, very effectively suppressed unwanted radiation as demonstrated by the following tests. Since absorption in H_2 at 600 cm^{-1} is relatively intense, a simple test for false radiation was obtained by noting the absence of energy transmitted at sufficiently high pressures of H_2. Another test was to show that the absorption coefficient is proportional to the square of the density, which must be true at the densities used.

The grating was calibrated primarily with lines at 698.7 and 906.7 cm^{-1} in a thin film of polystyrene[7] and was also checked against a water-vapor line at 525.98 cm^{-1}[8] and the Q-branch of the 15μ CO_2 band.[9] As a result of these calibrations, we feel that the frequency is known to ± 0.5 cm^{-1} in the region 500–900 cm^{-1}.

We noted in working with the grating blazed at 620 cm^{-1} that the grating angle at zero order (mirror angle) depended to a very small extent on the slit width, a variation which could have given an error in frequency measurements less than 1 cm^{-1}. This difficulty was corrected by realigning the monochromator, a procedure which did not change the grating calibration or previously measured values of the absorption coefficient. If the problem noted above was present in measurements at the lower frequencies, the error would be much less than 1 cm^{-1} and within the accuracy of the grating calibrations.

(b) *Gas cells*

To avoid instrumental drifts over the long periods of time required to obtain the data, a method was devised for inserting a reference cell identical to the test cell between the monochromator and the bolometer.[10] These cells were fabricated from 1.3 cm i.d. brass pipe 3.0 m long and were thoroughly cleaned and polished. For measurements in the region 10–600 cm^{-1}, the cells were terminated with high-density polyethylene windows. The method of obtaining a seal with such windows at high pressure and low temperature is described elsewhere.[11]

The transmission coefficient of high-density polyethylene in the region 50–350 cm^{-1} is given in Ref. (12). We made observations at room temperature from 350 to 600 cm^{-1} and found that a 4.8 mm thick sample has a transmission coefficient of about 45% at 415 cm^{-1}, 35% at 530 cm^{-1} and 25% at 560 cm^{-1}. This decrease in transmission is due to the onset of an intense band at 720 cm^{-1}.[13] Windows 3.2 cm thick were used for pressures up to 20 atm, 4.8 mm thick windows were used to 40 atm, and 6.4 mm thick windows to 100 atm. Despite the rapidly increasing attenuation of the polyethylene windows in the region above 500 cm^{-1}, it was convenient to obtain data over the wide range 10–600 cm^{-1} without changing windows. To operate satisfactorily above 500 cm^{-1}, however, the high density polyethylene windows were replaced by KRS–5 windows whose transmission coefficient is roughly 60% in the region 500–1000 cm^{-1}. This value depends on the perfection of the surface polish and varied for the windows that were on hand. Windows which were 2.5 cm in diameter, one pair 1.3 cm thick and the other 0.78 cm thick, were sealed respectively to the test and reference light pipes by a modification of the technique described in Ref. (3). A low-temperature-resistant silicone rubber cement (MBO130–119) and a primer (MBO125–050) developed by the Space Division, Rockwell International, were used to bond the windows to the metal wall terminating the light pipe. To seal the light pipe from the external environment, a high-density polyethylene disk 7.6 cm diameter with a 2.8 cm diameter hole to make room for the KRS-5 window and a brass ring concentric with the window were compressed between two flanges.[11] The ring prevented the polyethylene disk from exerting any pressure on the window and breaking its seal to the metal surface.

The KRS-5 windows were used at 195 K, but at 77 K leaks developed through the cement sealing the window to the metal flange. Because of this difficulty and because we had learned from Harshaw that KRS-5 may undergo a phase transition in the vicinity of 77 K which makes it opaque, we used instead 2.5 cm diameter CsBr windows, 1.3 cm thick and with a transmissivity of close to 90%. Because CsBr is softer than KRS-5, thicker CsBr windows had to be used.

The two light pipes were contained in a sheet metal box (3.3 m long, 30 cm wide, 12 cm high) externally lined with Dow Styrofoam for thermal isolation. A 25 cm section of vacuum-jacketed

light pipe, made of an inner thin-walled stainless steel tube (1.25 cm i.d. and gold plated), connected the 3 m gas cells in the bath to external light pipes. These transfer sections provided thermal isolation to obtain a uniform temperature within the gas cells. To stabilize the temperature of the gas and reference cells at room temperature, the bath was filled with water. A temperature of 195 ± 0.3 K measured by iron-constantan thermocouples was obtained by packing a methanol bath with solid CO_2. By filling the bath with liquid N_2, a temperature close to its boiling point 77.4 K was obtained. The level of liquid N_2 in the bath was maintained for long periods of time by a tank of liquid N_2 connected to the bath through a solenoid valve (I.T.T.) actuated by a temperature sensor and automatic controller. About 120 liters of liquid N_2 boiled away during a twelve hour period.

(c) *Bolometer*

To operate at frequencies above 500 cm^{-1}, it was necessary to remove the black polyethylene film in front of the cooled bolometer[6] because of its absorption. However, to avoid unnecessary heating of the bolometer and to provide additional filtering for the monochrometer, an OCLI low-pass filter L10928–9 with a sharp cut-off at 900 cm^{-1} was mounted in front of the bolometer.

(d) *Gases*

The H_2 gas was Matheson's ultra high purity grade (99.999% minimum purity). Possible contaminants are N_2, O_2, CO_2, CO, CH_4 and H_2O. The He used in the reference cell was Matheson's 99.9999% pure with the following contaminants: Ar, N_2, O_2, Ne, H_2, CO_2, CH_4, H_2O. Two tanks of an H_2–He mixture were obtained from Matheson and consisted of ultra high purity H_2 and Matheson grade He. At 292 and 195 K, an H_2–He mixture containing 35.15 mole % of H_2 was used, whereas at 77 K a mixture containing 31.72 mole % of H_2 was used. These analyses were made by gas chromatography. The concentrations of the various impurities appeared to be too small to affect absorption measurements significantly. The gas pressure was measured by Helicoid pressure gauges (ACCO) with ranges 0–20, 0–50 and 0–100 atm and a stated accuracy of 1/4 of 1% at full scale.

The gas-handling system and the arrangement for producing equilibrium H_2 is illustrated schematically in Fig. 1. Low temperature valves (Control Components ES 6000 series) were inserted in the gas lines located in the bath. To avoid leaks that developed at the connection of the external stem to the base, this joint was welded. The entire system was tested for leaks with a Veeco He leak detector. No data were taken unless the entire gas system could be pumped to a pressure in the range of 10^{-4} μ.

(e) *Preparation of equilibrium* H_2

To obtain an equilibrium ortho-para mixture of H_2, a catalyst was used which consisted of a nickel-silica granular powder (surface area approx. 500 m^2/g) called Apache 1 (Air Products and Chemicals). This catalyst was selected because it appeared to be the most effective, judged by the grams of H_2 converted per minute per gram of catalyst.[14,15] The catalyst was placed in a stainless steel tube (either 30 or 60 cm long) with 4 mm i.d. and was held in position by glass

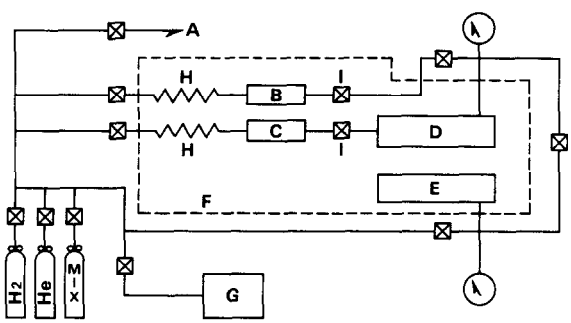

Fig. 1. Schematic diagram of the gas-handling system. A-exhaust, B-ortho-para catalyzer tube in removable lines; C-ortho-para catalyzer tube in permanently connected line, D-gas cell, E-reference cell, F-cryogenic bath, G-pump, H-cooling coil, I-low temperature valve.

wool plugs. Similar tubing was used to make a cooling coil preceding the catalyst tube to ensure that the gas would be cooled to the bath temperature before passing through the catalyst. The catalyst bed was prepared by heating it to approx. 140°C for about 2 hr in a gently flowing stream of He. Because such a bed was thought to be useful in removing residual H_2O and other impurities, the various gases used here were passed slowly through the Apache even at room temperature where H_2 is already an equilibrium ortho-para mixture.

3. EXPERIMENTAL CONSIDERATIONS

(a) *Method of determining the absorption coefficient*

If T_1 and T_2 are the transmissivities of light pipes 1 and 2 without any absorbing gas and I_1 and I_2 are the energies transmitted by light pipe 1 with absorbing gas and light pipe 2 empty, then the absorption coefficient is computed from[6]

$$\alpha = L^{-1} \ln \left(\frac{I_2 T_1}{I_1 T_2} \right), \tag{1}$$

where L is the length of each cell assumed to be equal. Since the energy transmitted by the light pipes were obtained within a minute or two of each other, the problem of a varying singal due to instrumental drift was virtually eliminated. However, over long periods of time, perhaps an hour or longer, a small drift in T_1/T_2 could appear due to a small leak in the light-pipe system or possibly from changes in the transmission of the stressed windows.

The ratio T_1/T_2 was determined at 5 cm^{-1} intervals with the gas cells filled with He to a pressure between 15 to 30 atm. Although the absorption in compressed He is zero in the i.r. region, a decrease in transmission of several percent was noted at roughly 5–10 atm of He attributable to the stressing and flexing of the high-density polyethylene windows. Beyond this pressure, there was apparently little further change in transmissivity. The change in transmissivity on stressing the CsBr windows with He was greater and did not appear to saturate as with the high-density polyethylene. Because of this pressure effect, we measured the tranmission of the test cell filled with the gas under study relative to the transmission of the same cell filled with He to comparable pressures. Unless such precautions are taken, errors in the absorption coefficient of 10% or more may occur.

The integration time was varied according to the signal-to-noise ratio, but typically four readings were taken at a given frequency, each with an integration time of 10–15 sec. The gas pressure in the test cell was adjusted so that I_2/I_1 remained between 0.2 and 0.6 to keep the fractional error in determining the absorption coefficient at a minimum.[6]

(b) *Spectral slit width*

The spectral resolution from 900–600 cm^{-1} was maintained in the range 15–10 cm^{-1} and was kept at roughly 10 cm^{-1} to 200 cm^{-1}. The spectral resolution at lower frequencies improved with decreasing frequency because the maximum slit width was determined by the diameter of the light pipe.

Since the spectral features in this study are of the order of 100 cm^{-1} or more wide, it is easy to ascertain that the distortion of the true profile due to these slit widths is negligible.[16,17] A useful relation between the true spectrum, $\phi(\nu)$, and the observed spectrum $\alpha(\nu)$, is given by[17]

$$\phi(\nu) = \alpha(\nu) - \frac{S^2}{12} \frac{d^2\alpha(\nu)}{d\nu^2} + \frac{S^4}{240} \frac{d^4\alpha(\nu)}{d\nu^4} - \cdots, \tag{2}$$

provided the series is rapidly convergent. This is the case when $S/\Delta\nu_{1/2} < 1$, where $\Delta\nu_{1/2}$ is the half width of the spectral line and S is one half the base of the slit function assumed to be triangular. From the conditions of this experiment, it is easy to show that $[\phi(\nu) - \alpha(\nu)]/\phi(\nu) < 0.01$.

(c) *Effective path length*

A small correction should be applied to the absorption coefficients obtained here to account for the fact that the effective path length, L_{eff}, is greater than the length of the gas cell, L,

because of the multiple reflections of the skewed rays from the wall of the light pipe. An expression for L_{eff} may be obtained by calculating the path length of a ray making an angle θ with the axis of the light pipe weighted by the reflection coefficient for perpendicularly polarized radiation, which is attenuated by reflections much less than the parallel component.[18] The result is

$$\frac{L_{\text{eff}}}{L} = 1 + \frac{8}{\theta_m^2} \frac{(\exp \zeta) - 1 - \zeta}{\zeta[(\exp \zeta) - 1]} \tag{3}$$

where θ_m is the maximum grazing angle made by the incoming radiation, i.e. $\theta_m = f/2$, where f is the f/number of the radiation. The parameter ζ is defined by $\zeta = XL/2df^2$, where d is the diameter of the light pipe and $X = 0.18(\rho/\lambda)^{1/2}$, ρ is the resistivity in ohm-cm and λ is the wavelength in cm. The speed of the monochromator is estimated to be $f/3.8$.[6] However, the f-number of the radiation entering the gas cell was more like $f/1.9$, since the radiation exiting through a 2.54 cm long slit was transmitted through a cone[19] to a light pipe 1.27 cm diameter. Then, for $\rho = 18 \times 10^{-6}$ ohm-cm which is the value measured for brass light pipes,[18] we find approx. $L/L_{\text{eff}} = 1.016$ in the region 10–600 cm^{-1}, and the absorption coefficients should be reduced by 1.6%. Since we later removed the light cone because it introduced excessive losses in the system rather than increasing the throughput as intended, the path-length error is even less.

(d) *Ortho-para conversion*

Comparisons at 78 K of $\alpha(370\ \text{cm}^{-1})$ at the peak of the $S(0)$ line with H_2 admitted directly to the gas cell or first passed slowly through a catalyst tube 1.5 cm i.d., 1 m long, prepared by heating the Apache to temperatures less than 373 K, revealed incomplete ortho-para conversion. However, satisfactory conversion was obtained by heating the Apache to 413 K while gently flowing He for about two hours in a smaller diameter tube (1.4 cm i.d.) to promote better mixing, although these tubes were shorter (30 or 60 cm long).

Many absorption measurements were made at 370 and 600 cm^{-1} for various flow rates of H_2 through the Apache tube. Although differences were noted, there was no trend in the values of α for filling rates between 2 and 0.25 atm/min. Only for rates distinctly in excess of 2 atm/min was there evidence for incomplete conversion. At a flow rate of 1 atm/min, the value that was more or less used, the rate normalized to the weight of Apache was 0.082 gH_2/min/g Apache. For a flow rate at 78 K of 0.124 in the same units, complete ortho-para conversion, as determined by thermal conductivity measurements, has been reported.[14] The equilibrium value of 50.7% parahydrogen was observed to decrease by 1% when the flow rate was doubled.

After air had been accidentally admitted to the Apache tube, measurements in the range 530–600 cm^{-1} at 78 K revealed that the Apache was poisoned since the absorption coefficient of H_2 was 10–15% higher. However, another properly processed Apache tube was connected into the system and lower values of α were obtained, in reasonable agreement with those observed before the poisoning.

In producing eH_2 in an H_2–He mixture by flowing the gas through the catalyst tube, the possibility of a change in the concentration of H_2 by preferential adsorption of H_2 must be considered. At 77 K, roughly 300 cc of H_2 at STP are adsorbed per gram of charcoal or 50 cm^3 of STP H_2 per gram of silica gel, since the amount of H_2 adsorbed in silica is roughly six times less than on charcoal at the same temperature and pressure.[20] This estimate assumes that the adsorption bed operates at 100 atm and that the partial pressure of H_2 is 33 atm. Since the volume of our gas cell is 380 cm^3 and 1.4 g of catalyst were used, we find that the amount of H_2 required to saturate the catalyst is contained in less than 0.1 atm of the H_2–He mixtures used, indicating that adsorption of H_2 by the catalyst at 77 K should not be significant. In any event, the catalyst bed was prepared by flowing H_2–He to saturate the catalyst with H_2 before admitting the mixture to the test cell.

4. RESULTS

The absorption coefficients per amagat^2 of eH_2 and eH_2–He in the region 10–900 cm^{-1} at 77.4, 194.7 and 292.4 K, determined every 5 cm^{-1}, are shown in Figs. 2–4 respectively. Two lines

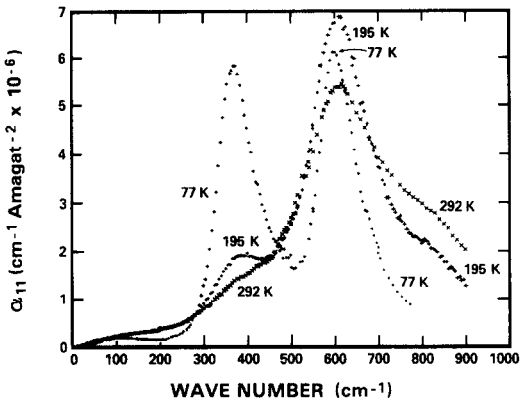

Fig. 2. The spectrum from 20 to 900 cm^{-1} of equilibrium H_2, α_{11} (cm^{-1} amagat$^{-2} \times 10^{-6}$), at 77.4, 194.7 and 292.4 K.

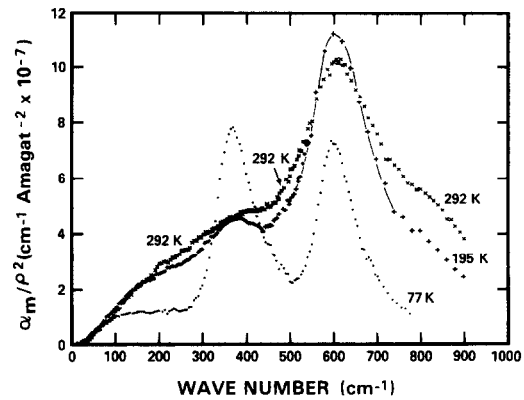

Fig. 3. The spectrum from 20 to 900 cm^{-1} of equilibrium of H_2–He mixtures, α_m/ρ^2 (cm^{-1} amagat$^{-2} \times 10^{-7}$), at 77.4 K (31.7 mole per cent H_2), 194.7 K (35.2 mole per cent H_2) and 292.4 K (35.2 mole per cent H_2).

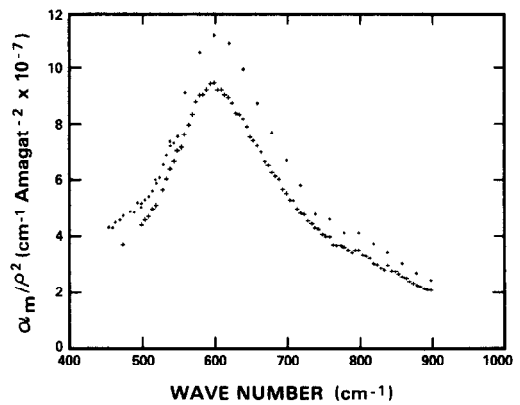

Fig. 4. The spectrum from 500–900 cm^{-1} of equilibrium H_2–He mixtures, α_m/ρ^2 (cm^{-1} amagat$^{-2} \times 10^{-7}$) at 194.7 K, upper spectrum 35.2 mole per cent H_2, lower spectrum 31.7 mole %H_2.

$S(0)$ at roughly 370 cm^{-1} due to the $J_1 = 0$ to $J_1 = 2$, $\Delta J_2 = 0$ transition, and $S(1)$ at 600 cm^{-1} due to the $J_1 = 1$ to $J_1 = 3$, $\Delta J_2 = 0$ transition, are resolved particularly at the lower temperatures. The $J_1 = 2$ to $J_1 = 4$, $\Delta J_2 = 0$ transition, $S(2)$, at 810 cm^{-1}, can be seen as a distortion of the high-frequency wing. The low-frequency results for eH_2 are replotted with an expanded scale (10X) in Fig. 5 to emphasize the translational band ($\Delta J_1 = \Delta J_2 = 0$) which peaks in the neighborhood of 100 cm^{-1} but extends to much higher frequencies. The spectrum of eH_2–He at 195 K from 500 to 900 cm^{-1}, plotted every 5 cm^{-1} for a mixture containing 31.7 mole % H_2 and, for comparison, the results for the 35.2 mole % H_2 mixture are shown in Fig. 5. The average

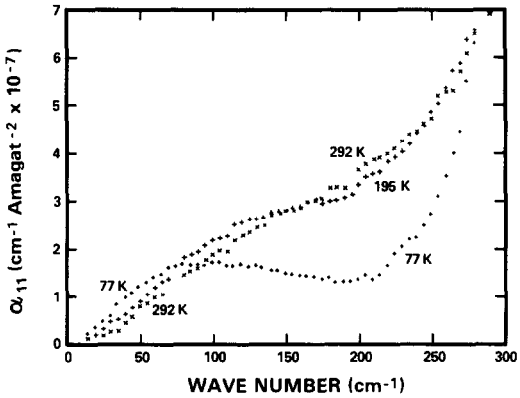

Fig. 5 The low -frequency portion of the spectrum of equilibrium H_2 emphasizing the translational band, α_{11} (cm^{-1} amagat^{-2} x 10^{-7}), at 77.4, 194.7 and 292.4 K.

deviation of the points from a smooth curve through the data points is less than 1% in all the figures.

Pressures in the range 10–100 atm were used to maintain the transmissivity of the gas between 0.2 and 0.6 to minimize the fractional error in determining α.[6] The equations and constants used to compute the amagat density from pressure measurements are given in Table 1. A number of measurements of absorption coefficients as functions of density at different temperatures and frequencies for H_2 and H_2–He mixtures showed that, within experimental error, α is proportional to the density squared in the pressure range used. The greatest pressure used was 100 atm.

Results in the region 525–600 cm^{-1}, obtained with a 500 cm^{-1} grating and gas cells terminated by high-density polyethylene windows, tended to be greater by 5–15% than those obtained with the 750 cm^{-1} grating and gas cells terminated by CsBr windows. Although the signal-to-noise ratio was poor with the high-density polyethylene windows because of their high absorption in this region, this could not account for such a systematic difference. We believe that this discrepancy was due to false radiation produced by the rather poor surface finish of the 500 cm^{-1} grating. In view of this, we have discarded the results obtained with this grating from 550 to 600 cm^{-1}. Since this grating was used for lower frequency measurements, further

Table 1. The density in amagat, $\rho = \rho_{p,T}/\rho_{NTP}$, where $\rho_{p,T}$ is calculated from the pressure, p, in atm by

$$\rho_{p,T} = p[A + Bp + Cp^2]^{-1}$$

where $A = 3.661 \times 10^{-3}$ T atm/amagat and B and C are given in the table below. $B(H_2\text{–He})$ for the mixture is computed from

$$B(H_2\text{–He}) = x_1^2 B_{11} + (1-x_1)^2 B_{22} + 2x_1(1-x_1)B_{12},$$

where x_1 is the mole fraction of H_2. Values of $B(H_2\text{–He})$ for $x = 0.352$ is given in the table.

T (K)	A atm amagat^{-1}	B_{11} amagat^{-1} x 10^{-4}	$B(H_2\text{–He})$ amagat^{-1} x 10^{-4}	C_{11} (atm amagat)$^{-1}$ x 10^{-6}
292.2	1.073	6.56[a]	6.38[a]	-
194.7	0.714	4.71[b]	7.32[b]	-
77.4	0.2832	-4.47[c]	3.17[d]	3.17[c]

[a] C. W. Gibby, C. C. Tanner, and I. Masson, Proc. Roy. Soc. (London) 122, 283 (1929).

[b] J. Brewer and G. W. Vaugh, J. Chem. Phys. 50, 2960 (1969).

[c] J. H. Dymond and E. B. Smith, "The Virial Coefficient of Gases," p. 158, Table 1, Clarendon Press, Oxford (1969).

[d] Computed from E. A. Guggenheim and M. L. McGlashan, Proc. Roy. Soc. (London) A206, 448 (1951).

measurements were made with a new 500 cm^{-1} grating whose surface finish was very good. The values of absorption coefficient obtained with the new grating were indistinguishable from the previous values in the region 350–550 cm^{-1}.

The absorption α_{12} (cm^{-1} $amagat^{-2}$) for H_2–He collisions is given in Fig. 6. The quantity α_{12} is computed from

$$\alpha_m = \alpha/\rho^2 = x(1-x)\,\alpha_{12} + x^2\alpha_{11}, \tag{4}$$

where α is the absorption coefficient of the mixture, ρ is the total density equal to $\rho_1+\rho_2$, $x = \rho_1/\rho$, α_{11} is due to H_2–H_2 collisions (Figs. 2 and 5), and α_m is due to the mixture (Figs. 3 and 4). To obtain the points in Fig. 6, seven values of α_{11} (Fig. 2) spanning a frequency interval of 30 cm^{-1} were fitted by a smooth curve to provide a point corresponding to the mixture data in Fig. 3. The oscillations in α_{12}, which can be seen with smaller amplitude in α_m (Fig. 3), are likely due to some systematic error. Similar oscillations have been observed in a previous investigation [Ref. (21), Fig. (11)].

The error in the reduced spectrum α_{12} may be considerably greater than that in α_m or α_{11}. To show this, we obtain from eqn (4), by the method of propagating precision indices,

$$\epsilon_{12} = \frac{\Delta\alpha_{12}}{\alpha_{12}} = \epsilon\left(1 + \frac{2x}{1-x}\,\frac{\alpha_{11}}{\alpha_{12}}\right), \tag{5}$$

where we have taken $\Delta\alpha_m/\alpha_m = \Delta\alpha_{11}/\alpha_{11} = \epsilon$. We see from Figs. 2 and 6 that $\alpha_{11} \gg \alpha_{12}$, except in the translational band where $\alpha_{11} < \alpha_{12}$. Where $\alpha_{11} \gg \alpha_{12}$, a very small value of x (a very dilute H_2 mixture) is required to obtain accurate values of α_{12}. However, our major interest was in obtaining accurate values for α_{12} in the translation band and here the mixture ratios used are adequate. The inequality $\alpha_{11} \gg \alpha_{12}$ holds because the polarizability of H_2 is much greater than that of He. However, in the translational band, $\alpha_{12} > \alpha_{11}$ because in collisions between H_2 and He an isotropic overlap induction is operative.

We next compare our results with those of other investigators. In the bandwidth quoted, values of α/ρ^2 are compared every 50 cm^{-1}. Since the results for H_2 obtained with a Michelson type interferometer by BOSOMWORTH and GUSH[21] are thought to be reliable, it is gratifying that our results are in such good agreement. In the region 50–440 cm^{-1}, the results of BOSOMWORTH and GUSH[21] at 300 K agree with ours at 292.4 K on the average within 2.5%. It should be noted that the effect of somewhat different temperatures on α/ρ^2 is rather small. For normal H_2 at 77.4 K in the region 100–450 cm^{-1}, our results agree to within 4.5%.

CUNSOLO and GUSH[22] measured the absorption in H_2 at room temperature with a lamellar grating interferometer from 4 to 50 cm^{-1} and found a sudden drop in the absorption below 10 cm^{-1}, which they attributed to the reversal of the dipole moment in successive collisions, as discussed by VAN KRANENDONK.[23] At 50 cm^{-1}, we agree within 3% with the results of CUNSOLO and GUSH[22] whereas, at 25 cm^{-1}, where the error in the present results is greater because of

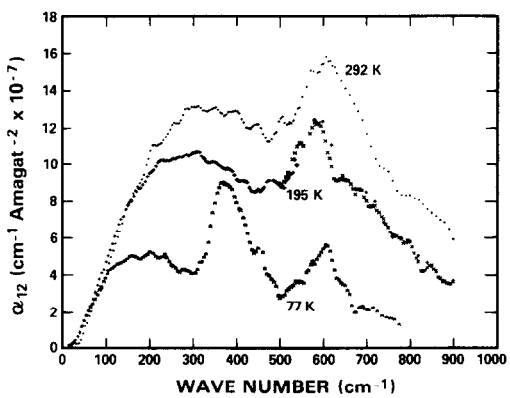

Fig. 6 The reduced spectrum from 10–900 cm^{-1} of equilibrium H_2–He, α_{12} (cm^{-1} $amagat^{-2} \times 10^{-7}$) at 77.4, 194.7 and 292.4 K.

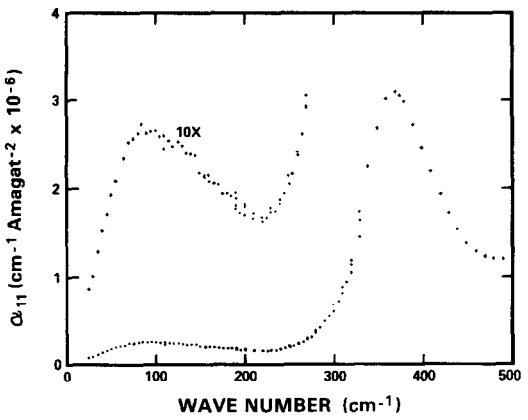

Fig. 7 The spectrum from 10 to 500 cm^{-1} of normal H_2, α_{11}, at 77.4 K. The upper spectrum is the same as the lower spectrum multiplied by factor of 10.

smaller absorption, the agreement is poorer, namely, 20%. DAGG *et al.*[24] measured the microwave absorption in H_2 at 2.3 cm^{-1} and obtained a value very much greater than that implied by the data of CONSOLO and GUSH,[22] a result which does not support their observation of a decisive dip. Our value of absorption in the region 25–75 cm^{-1}, extrapolated to 2 cm^{-1} and ignoring the possibility of the dipole-reversal dip, is about 40% less than that of DAGG *et al.* However, the possibility of impurity absorption cannot be discounted since they did not report any special effort to purify the H_2.

The present results on H_2 at 292.4 K from 550 to 900 cm^{-1} are greater than those of KISS *et al.*[3] at 300 K by 8%, and greater than their results as presented by BOSOMWORTH and GUSH[25] by 13%. In the same wavelength region, the present H_2 results at 292.4 K and those of MACTAGGART and HUNT[4] at 298 K agree within 6% if we use their more accurate results obtained with the long cell. Our results for H_2 at 292.4 K agree closely with those of COPLA and KETELAAR[5] at 298.2 K in the range 450–900 cm^{-1}; the average deviation is in the neighborhood of 3%. At 195 K, our results are greater than those of MACTAGGART and HUNT[4] by 14% and greater than those of KISS *et al.*[3] on the average by 8% in the region 550–900 cm^{-1}. A few per cent of this difference may be attributed to the fact that these investigators worked with n–H_2 whereas we worked with e–H_2. The results of MACTAGGART and HUNT[4] and of KISS *et al.*[3] differ, on the average, by 15%. Although there are many possibilities for experimental error which could account for the above discrepancies, window distortion due to pressure is one that comes to mind since none of the previous investigators noted this effect nor reported taking any measures to deal with it. In the frequency region under consideration, discrepancies of ± 10% between the results of different investigators is certainly not unusual. However, we shall see that errors of this magnitude can propagate into much larger errors in evaluating small contributions to the intensity of the spectra.

At 77.4 K where the rotational lines are relatively well resolved, the peak frequency of the $S(0)$ line is observed at 368 cm^{-1} and the $S(1)$ line at 598 cm^{-1}. As noted previously,[3,25] these lines appear at higher frequencies than the Raman frequencies for the free molecule, namely at 354.4 and 587.1 cm^{-1}, respectively.[27] The shift of the peak of the $S(1)$ line with increasing temperature has the same origin as the shift in the Raman frequencies, namely, the effect of frequency-dependent Boltzmann factors.[26] The increasing width of the rotational lines with increasing temperature is due to the decrease in duration of collision because of the increase in mean relative velocity.

The most striking difference between the H_2 (Fig. 2) and H_2–He (Figs. 3 and 6) spectra is the greatly enhanced translational band in the latter. This is due to induced dipoles arising from the spherical part of the overlap interaction in H_2 and He collisions which, however, is forbidden in the rotational transitions.[28,29] Because of the shorter range of the overlap compared with the quadrupolar interaction, the translational band due to H_2–He collisions extends to higher frequencies than for H_2–H_2 collisions.

The translational band of n–H_2 at 77 K shown in Fig. 7 appears to be qualitatively similar to that of e–H_2, except for the greater amplitude of the former. This increase is expected since the

concentration of ortho molecules which possess a quadrupole relative to those in state $J = 0$ which are spherically symmetric is greater in n–H_2. For molecules in the state $J = 0$, the translational transitions $\Delta J_1 = 0$ is forbidden.

5. THR INTEGRATED INTENSITY

In this section, we present experimental values of the spectral invariants α_1 and γ_1 given by

$$\alpha_1 = n^{-2}\int \alpha(\omega)\, d\omega, \tag{6}$$

$$\gamma_1 = n^{-2}(\beta\hbar/2)\int \frac{\alpha(\omega)d\omega}{\omega\tanh(\beta\hbar\omega/2)}, \tag{7}$$

where n is the number density, ω the angular frequency, $\beta = (kT)^{-1}$, and the integrals are taken over the entire rotational-translational band. These values of α_1 and γ_1 are compared with theoretical values computed from[30,31]

$$\alpha_1 = \frac{2\pi\alpha^2}{Ic}6q_2\frac{\theta^2}{\sigma^5}\left[I_8 + 2\left(1+\frac{\kappa}{5}\right)A_\kappa I_{8+\kappa} + \frac{6+(\kappa+3)^2}{15}A_\kappa{}^2 I_{8+2\kappa}\right.$$
$$+\frac{14}{3}\frac{I}{m\sigma^2}\left(I_{10} + 2\left(1+\frac{\kappa}{5}\right)\left(1+\frac{\kappa}{7}\right)A_\kappa I_{10+\kappa}\right.$$
$$\left.\left.+\left(1+\frac{24}{35}\kappa+\frac{38+(\kappa+7)^2}{420}\kappa^2\right)A_\kappa{}^2 I_{10+2\kappa}\right)\right], \tag{8}$$

$$\gamma_1 = \frac{2\pi^2\overline{\alpha^2}q_2}{ckT}\frac{\theta^2}{\sigma^5}\left[I_8 + 2\left(1+\frac{\kappa}{5}\right)A_\kappa I_{8+\kappa} + \frac{6+(\kappa+3)^2}{15}A_\kappa{}^2 I_{8+2\kappa}\right]. \tag{9}$$

Here θ is the quadrupole moment, I is the moment of inertia, m is the reduced mass, σ is the molecular diameter, $\overline{\alpha^2}$ is the mean square polarizability, and $q^2 = 1 - 2(\alpha_\parallel - \alpha_\perp)^2/15\overline{\alpha^2}$. The anisotropic term, which is very small for H_2, gives the contribution to α_1 for transitions in which both molecules change rotational state. The I_n functions are defined by

$$I_n = 4\pi\int_0^\infty g(x)x^{-n}x^2 dx, \tag{10}$$

where $g(x)$ is the pair distribution function.

The term in eqn (8) multiplied by the factor $I/m\sigma^2$ is the translational contribution to α_1. The terms containing A_κ in eqns (8) and (9) are the contributions from the interference between the dipoles induced by the quadrupole and anisotropic overlap fields. The terms containing $A_\kappa{}^2$ are due to the anisotropic overlap interaction, a much smaller contribution than the former. Omitted from these expressions are terms due to the dipole induced by the hexadecapole moment, Φ. However, using the upper limit for the value of Φ for H_2 recently determined by GIBBS *et al.*[32] we find that the hexadecapole contribution to γ_1 at 292 K is only 0.2% of the quadrupole contribution.

From the data of Fig. 2, we evaluate eqns (6) and (7) in the region 0–900 cm^{-1}. To obtain the contribution in the rest of the high-frequency wing from 900–1600 cm^{-1}, we use the data of MACTAGGART and HUNT[4] at room temperature and 195 K adjusted to agree with our data in the region 800–900 cm^{-1}. As expected, the contribution of the high-frequency wing is less for γ_1 than α_1. Except for α_1 at 292 K and 195 K, where the absorption in the region 900–1600 cm^{-1} amounts to 28 and 14% of the total, respectively, this high-frequency contribution to α_1 at 77 K and to γ_1 is appreciably less than 10%. The contribution to α_1 and γ_1 from absorption in the region 900–1600 cm^{-1} was estimated by using the empirical power-law shape of MACTAGGART and HUNT[4]. The experimental values of α_1 and γ_1 obtained this way are shown in Table 2.

Theoretical values of α_1 and γ_1, with the overlap terms taken to be zero ($A_\kappa = 0$), were computed from eqns (8) and (9) with the following values of the molecular constants:

Table 2. Experimental values of α_1 (6) and γ_1 (7), theoretical values (quadrupole contribution only) of α_1 (8) and γ_1 (9), and experimental and theoretical values of $\alpha_1 I/\gamma_1 kT$ (11).

	α_1 10^{-31} s^{-1}cm^5		γ_1 10^{-58} s cm^5		$\alpha_1 I/\gamma_1 kT$	
T(K)	exp.	theor.	exp.	theor.	exp.	theor.
292.4	6.88	5.29	1.12	0.91	7.17	6.79
194.7	5.84	4.86	1.46	1.26	7.01	6.76
77.4	4.84	4.42	2.92	2.90	7.31	6.72

$I = 4.714 \times 10^{-4}\ g\ cm^2$ ($I = h/8\pi^2 cB$ with $B = 59.331\ cm^{-1}$),[27] $\alpha_\parallel = 0.934 \times 10^{-24}\ cm^3$, $\alpha_\perp = 0.718 \times 10^{-24}\ cm^3$,[33] $\theta = 0.662 \times 10^{-26}$ esu cm^2,[34] $\sigma = 2.92 \times 10^{-8}$ cm, and $\epsilon/k = 36.8$ K.[35] At 292 and 195 K, the function I_8 was evaluated from eqn (10), where the classical distribution function was used and quantum corrections[28,36] were applied. These corrections are negative and amount to 2.6% and 4.0% of the classical values, respectively, at 292 and 195 K. At 77.4 K, the series expansion for the quantum correction to the classical pair-distribution function is unreliable and an accurate calculation of the quantum value of $g_{qu}(R)$ must be used. Using the values of $g_{qu}(R)$ obtained by POLL and MILLER[37] at 80 K, we find that $I_8(qu) = 3.640$ compared with $I_8(cl) = 4.117$ at 80 K. The value of $I_8(qu)$ at 77.4 K is practically the same as that at 80 K. The theoretical values of α_1 and γ_1 shown in Table 2 were obtained with $I_8(qu)$ at 80 K.

Table 2 shows that except at 77.4 K the experimental values of α_1 and γ_1 are larger than the theoretical values. Table 3 shows that these differences are in the range 10–20% except at 77.4 K where the difference for γ_1 of essentially zero may reflect some experimental error. The differences between experimental and theoretical values of α_1 and γ_1, computed on the basis of quadrupole induction alone, have been attributed to an anisotropic overlap interaction.[28] VAN KRANENDONK and KISS[28] and COLPA and KETELAAR[38] find that this overlap contribution should be, respectively, 11 and 21% of the experimental values at room temperature. For the integrated absorption $\int \alpha(\nu)\, d\nu/\nu$ associated with the $S(1)$ line, POLL and HUNT[39] find the difference between experiment and theory based on the quadrupole interaction alone to be 53%, which is much larger than that obtained in any other investigation. However, it is difficult to compare the various estimates of this difference, not only because of variations in experimental results, but also because different molecular constants were used in the calculations. If we were to use $\sigma = 2.98$ Å, the value adopted by POLL and HUNT,[39] instead of 2.92 Å, the portions of α_1 and γ_1 attributable to an overlap interaction would be larger than given in Table 3 but still not nearly as great as those given by these authors.

On taking the ratio of eqns (8) and (9), we obtain, ignoring the overlap terms,

$$\frac{\alpha_1 I}{\gamma_1 kT} = 6\left(1 + \frac{14}{3}\frac{I}{m\sigma^2}\frac{I_{10}}{I_8}\right). \tag{11}$$

The values of $\alpha_1 I/\gamma_1 kT$ given by eqn (11) are shown in Table 2 and found to be somewhat less than the experimental values. An examination of eqns (8) and (9) reveals that inclusion of a

Table 3. Fractional difference between experimental and theoretical values of α_1 and γ_1.

T(K)	$\frac{\alpha_1(\text{exp})-\alpha_1(\text{theor})}{\alpha_1(\text{exp})}$	$\frac{\gamma_1(\text{exp})-\gamma_1(\text{theor})}{\gamma_1(\text{exp})}$
292.4	0.23	0.19
194.7	0.17	0.14
77.4	0.09	0.007

small overlap term would only slightly increase the values of $\alpha_1 I/\gamma_1 kT$. The fact that calculated values of $\alpha_1 I/\gamma_1 kT$ are slightly less than the experimental value signifies that the contribution of multipoles higher than the quadrupole to the induced absorption is quite small.[26] This is in accordance with the fact that the contribution to γ_1 by hexadecapolar induction is only 0.2% of the quadrupolar induction.

6. CONCLUSION

We have determined the far-i.r. absorption in H_2 and H_2–He at several temperatures over a broad frequency range and have attempted to establish the accuracy of these results by considering the various sources of experimental error. The major portion of the spectral moments can be accounted for by quadrupole-induced dipoles. Although the remainder can be attributed to an anisotropic, overlap-induced dipole, its accurate determination depends on the values of the molecular parameters, particularly the molecular diameter. If the overlap interaction could be evaluated theoretically, the data and analysis presented here could be used to obtain an accurate value for the molecular diameter.

Acknowledgements—The author thanks Mr. R. K. HORNE for assistance in obtaining the data, Dr. E. R. COHEN for assistance in reducing the data and a number of valuable discussions, and Dr. G. E. SCHMAUCH for advice on the use of the catalyst Apache.

REFERENCES

1. M. B. MCELROY, *J. Atmos. Sci.* **26**, 798 (1969).
2. L. M. TRAFTON, *Ap. J.* **146**, 558 (1966); **147**, 765 (1967).
2a. Preliminary results of this work in the region 20–600 cm^{-1} have been presented by F. W. TAYLOR and A. D. JONES III, *Icarus* **29**, 299 (1976).
3. Z. J. KISS, H. P. GUSH and H. L. WELSH, *Can. J. Phys.* **37**, 362 (1959).
4. J. W. MACTAGGART and J. L. HUNT, *Can. J. Phys.* **47**, 65 (1969).
5. J. P. COLPA and J. A. A. KETELAAR, *Molec. Phys.* **1**, 14 (1958).
6. I. F. SILVERA and G. BIRNBAUM, *Appl. Opt.* **9**, 617 (1970).
7. *Tables of Wavenumbers for the Calibration of Infra-Red Spectrometers*, pp. 682–683. International Union of Pure and Applied Chemistry, Butterworths, London (1961).
8. L. R. BLAINE, E. K. PLYLER and W. S. BENEDICT, *J. Res. NBS* **66A**, 223 (1962), H_2O line No. 16B.
9. The peak of the Q-branch is at 668.5 cm^{-1}; private communication by V. KUNDE. See also H. G. REICHLE, JR. and C. YOUNG, *Can. J. Phys.* **50**, 2662 (1972).
10. G. BIRNBAUM and I. F. SILVERA, *Infrared Phys.* **17**, 235 (1977).
11. R. K. HORNE and G. BIRNBAUM, *Infrared Phys.* **17**, 173 (1977).
12. R. V. MCKNIGHT and K. D. MOLLER, *J. Opt. Soc. Am.* **54**, 132 (1964).
13. E. K. PLYLER and L. R. BLAINE, *NBS J. Res.* **64C**, 55 (1960).
14. C. MCKINLEY and G. E. SCHMAUCH, *Adv. Cryogenic Engng.* **9**, 217 (1964).
15. G. E. SCHMAUCH and A. H. SINGLETON, *Ind. Engng Chem.* **56**, 20 (1964).
16. H. H. KOSTKOWSKI and A. M. BASS, *J. Opt. Soc. Am.* **46**, 1060 (1956).
17. I. R. HILL and D. STEELE, *Farad. Trans. II* **70**, 1233 (1974).
18. R. C. OHLMAN, P. L. RICHARDS and M. TINKHAM, *Opt. Soc. Am.* **48**, 531 (1958).
19. W. WITTE, *Infrared Phys.* **5**, 179 (1965).
20. The author is indebted to W. R. Parrish for these comments which are based on data given by A. J. KIDNAY and M. J. HIZA, *Adv. Crys. Engng* **12**, 730 (1967); *Cryogenics* **10**, 271 (1970).
21. D. R. BOSOMWORTH and H. P. GUSH, *Can. J. Phys.* **43**, 729 (1965).
22. S. CUNSOLO and H. P. GUSH, *Can. J. Phys.* **50**, 2058 (1972).
23. J. VAN KRANENDONK, *Can. J. Phys.* **46**, 1173 (1968).
24. I. R. DAGG, G. E. REESOR and J. L. URBANICK, *Can. J. Phys.* **53**, 1764 (1965).
25. D. R. BOSOMWORTH and H. D. GUSH, *Can. J. Phys.* **43**, 729 (1965).
26. G. BIRNBAUM and E. R. COHEN, *Can. J. Phys.* **54**, 593 (1976).
27. B. P. STOICHEFF, *Can J. Phys.* **35**, 730 (1957).
28. J. VAN KRANENDONK and Z. J. KISS, *Can. J. Phys.* **37**, 1187 (1959).
29. J. D. POLL and J. VAN KRANENDONK, *Can. J. Phys.* **39**, 189 (1961).
30. C. G. GRAY, *J. Phys. B: Atom. Molec. Phys.* **4**, 1661 (1971).
31. E. R. COHEN, *Can. J. Phys.* **54**, 475 (1976).
32. P. W. GIBBS, C. G. GRAY, J. L. HUNT, S. PADDI REDDY, R. H. TIPPINGS and K. S. CHANG, *Phys. Rev. Lett.* **33**, 256 (1974).
33. H. VOLKMANN, *Ann. der Physik* **24**, 457 (1935), quoted by J. O. Hirschfelder.
34. D. E. STOGRYN and A. P. STOGRYN, *Molec. Phys.* **11**, 371 (1966).
35. *American Institute of Physics Handbook*. pp. 4-122–4-129, McGraw-Hill, New York (1957).
36. J. VAN KRANENDONK, *Physica* **24**, 347 (1958).
37. J. D. POLL and M. S. MILLER, *J. Chem Phys.* **54**, 2673 (1971).
38. J. P. COLPA and J. A. A. KETELAAR, *Molec. Phys.* **1**, 343 (1958).
39. J. D. POLL and J. L. HUNT, *Can. J. Phys.* **54**, 461 (1976).